



# Heavy metal pollution from listwaenitization: In case of Alakeçi (Bayramiç - Çanakkale / West Türkiye)

Alaaddin Vural 

Gümüşhane University, Faculty of Natural Sciences and Engineering, Department of Geological Engineering, 29100, Gümüşhane, Türkiye

## Abstract

This study aimed to investigate the risk of element / heavy metal pollution caused by listwaenitization. In this context, the heavy metal pollution risk of listwaenite-derived soils in the region where listwaenitized ultrabasic rocks are present as a result of hydrothermal alterations in the vicinity of Alakeçi (Bayramiç Çanakkale / Western Türkiye) was investigated with pollution index, geoaccumulation index and integrated pollution risk parameters. For this purpose, Cu, Zn, Pb element concentrations of 350 soil samples collected from the field were determined, and Pollution Index (PI) and Geo-accumulation Index (Igeo) parameters for each element and Integrated Pollution Index (IPI) parameters for each sampling point were calculated. In addition, distribution maps of PI, Igeo and IPI parameters were plotted. When the site is considered in terms of IPI parameter, it has been determined that the site has medium and high pollution risk. When the field is considered in terms of PI and Igeo parameters, a remarkable level of pollution has been detected in the field, especially by Ni, Co and As elements. When the distribution maps of the PI, Igeo and IPI parameters are examined, it has been determined that the pollution risk is higher than the other areas, especially in the areas where hydrothermal alteration is intense and in the tectonic line areas. Although listwaenitizations and listwaenite zones are important target areas especially for epithermal gold mineralizations, this study has shown that listwaenitization areas are also areas at risk of heavy metal pollution. Therefore, listwaenitization zones are areas that should be investigated in terms of heavy metal pollution risk as well as epithermal gold mineralization potentials.

**Keywords:** Listwaenite / listwaenitization, heavy metal pollution, pollution Index (PI), integrated pollution index (IPI), geo-accumulation index (Igeo)

## 1. Introduction

The concept of listwaenitization / listwaenite was first used for the Ural gold fields of Russia located in the Livtenya region [1–3]. Although the concept of listwaenite entered the literature a long time ago, the associated mineralization models are still controversial [1,4–7]. However, the concept of listwaenite has been accepted by many researchers and has been used in many studies [1,8–16]. Listwaenite is a hydrothermal alteration process and the end products of the process are soil zones developed over listwaenitization zones [6,17,18]. Although listwaenitization zones are the subject of mineral exploration, they are also products of hydrothermal alteration, and as a result of alteration, some elements are enriched in the environment, while others are depleted. When evaluated in this context, the listwaenitization zones and the soil developments in

these zones may be exposed to metal enrichment / pollution. Metal enrichment in soils started to attract the attention of the society especially after the second quarter of the last century and many studies were carried out for this purpose [19–21]. Heavy metal pollution has many negative effects not only in the soil, but also in the aquatic environment, together with the food chain, and therefore on human health. [22,23].

The aim of this study is to investigate the risk of heavy metal pollution in developed soils over the Alakeçi (Bayramiç / Çanakkale - Western Türkiye) listwaenitization occurrences. Soil samples collected from the field for mineral exploration purposes in the past [2,22] were evaluated in terms of heavy metal pollution risk by using different pollution parameters in this study.

**Citation:** A. Vural, Heavy metal pollution from listwaenitization: In case of Alakeçi (Bayramiç-Çanakkale/West Türkiye), Turk J Anal Chem, 4(2), 2022, 94–102.

**\*Author of correspondence:** alaaddinvural@hotmail.com

**Tel:** +90 (456) 233 17 13

**Fax:** +90 (456) 233 10 75

**Received:** October 18, 2022

**Accepted:** November 21, 2022

## 2. Material and methods

### 2.1. Geological characteristics of the area

In the Biga peninsula, within the borders of Bayramiç (Çanakale-Türkiye) Alakeçi village and its vicinity, a listwaenitization development of approximately 1 km<sup>2</sup> is observed within the Alakeçi mylonitic zone [2,22,24]. The basement rocks of the region are Sakarya Zone, Ayvack-Karabiga Zone and Ezine Zone from southeast to northwest [24].

In the study area, Kazdağ Group metamorphics (consisting of gneiss, amphibolite, and marbles) (Sakarya Zone), ophiolitic mélangé (Ayvack-Karabiga Zone) and mylonitic gneiss unit and meta serpentinites (These two units are called Alakeçi Mylonitic zone) developed between these two zones are observed. All these units are cut by Tertiary magmatic rocks and covered by Tertiary volcanic and sedimentary rocks (Fig. 1 and 2a). The Alakeçi Mylonitic Zone formed between the ophiolitic mélangé and the Kazdağ Group is in east-northeast orientation in accordance with the main foliation of the Kazdağ Group [24]. Along this zone, 1.5–2 km long and approximately 400–500 meters wide, a listwaenite zone extends in the northwest-southeast direction and is interrupted by strike-slip faults in the northeast-southwest direction. (Fig. 1 and 2a). Listwaenite zone consists mainly of Fe-Mg carbonate, quartz, and fuchsite (mica mineral). These minerals are accompanied by scattered chromite and lesser amounts of pyrites. Listwaenite zone is covered with medium-well developed soil derived from listwaenites.

### 2.2. Sampling and analytical procedure

The study was carried out on 350 soil samples collected from the listwaenite zone and its vicinity, and the sampling and analytical procedure of the study are given in detail in the studies of [2] and [1]. Soil samples were taken from the B profile of the soil zone and from approximately 15–30 cm depths, from grid points equally spaced across the field. (Fig. 1, 2a). The collected samples were sifted through an 80 mesh sieve in accordance with routine sample preparation procedures

[25], dried in an oven at 60 °C for 24 hours to remove their natural moisture and analyzed by flame atomic absorption spectrometry (FAAS) for As, Sb, Cu, Pb, Zn, Ni and Co in at the General Directorate of Mineral Research and Exploration (MTA) Laboratory (Ankara-Türkiye). In the MTA Analysis, Technology and Calibration Laboratories, service is provided at the level and quality that meets the requirements of the TS EN ISO / IEC 17025 Standard, in accordance with the impartiality and confidentiality statements. MTA laboratory processes and MTA laboratory standards were used in the analytical procedures.

The method's accuracy has been proven by the analysis of standard reference materials. It was determined by the *t*-test that there was no statistically significant difference between the results obtained and the results were quite satisfactory ( $p \leq 0.05$ ) [26]. The precision of the method was evaluated with the relative standard deviation (RSD). RSD values for the studied elements were calculated to be between %1.2 (for Mo) and 3.2% (for Mo).

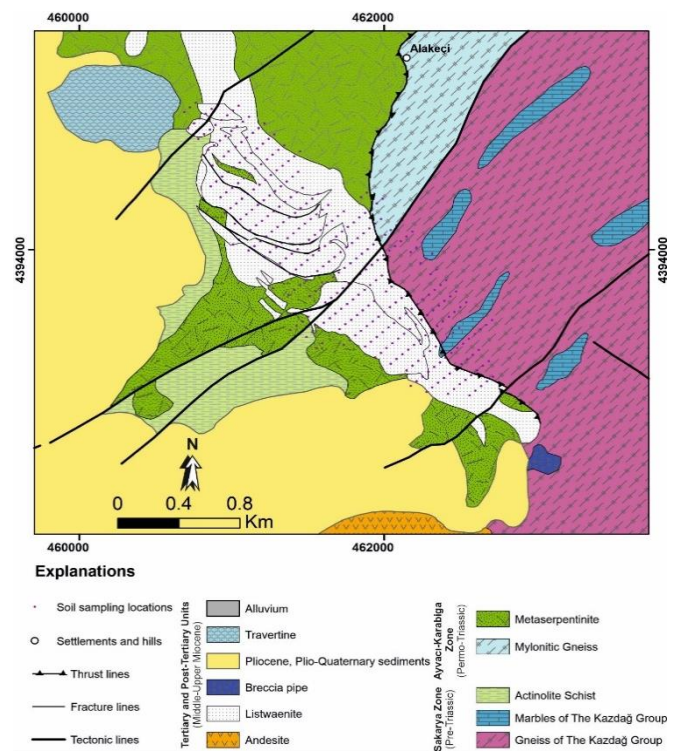


Figure 1. Geology of the study area and sampling map [1,2]

Table 1. Descriptive statistics of elements in soil samples

	Number*	Upper crust value**	Mean	Median	Geometric Mean	Minimum	Maximum	Standard deviation
Cu	342	28	38.3	33.0	32.9	10	265	29.1
Pb	340	17	24.4	20.0	22.3	10	90	10.4
Zn	342	67	64.2	55.0	58.3	15	545	38.8
As	325	4.8	93.3	50.0	61.4	5	800	86.1
Sb	220	0.4	4.8	4.0	3.5	2	60	6.2
Ni	340	47	1517.3	1250.0	916.5	10	6300	1271.1
Co	338	17.3	104.2	80.0	78.4	15	1255	98.1

\* It represents the number of samples measured above the detection limit for the element under investigation

\*\* Upper crust element concentrations from [33]

**Table 2.** Correlation coefficients of the elements

	Cu	Pb	Zn	As	Sb	Ni	Co
Cu	1						
Pb	0.42	1					
Zn	0.75	0.44	1				
As	-0.03	0.05	0.08	1			
Sb	0.08	0.06	0.12	0.65	1		
Ni	-0.26	-0.10	-0.01	0.36	0.18	1	
Co	-0.19	-0.03	0.02	0.37	0.20	0.73	1

### 2.3. Evaluation of the data

Statistical and spatial statistical evaluation of all data was evaluated with IBM SPSS 21 and ArcMap 10.8, respectively. Descriptive statistics and correlation coefficients of data belonging to 7 elements are given in [Tables 1 and 2](#) respectively.

Many different pollution parameters are used in the evaluation of heavy metal pollution [19]. In this study, Pollution Index (PI), Integrated Pollution Index (IPI) and Geo-accumulation Index (Igeo) parameters, which are the most well-known ones, were used to investigate heavy metal pollution in soils. The Pollution Index (PI) and the Integrated Pollution Index (IPI) are also widely used to assess media quality [27–31]. PI is obtained by dividing the element concentration in the soil with the average values in the upper crust and / or the earth's soil. In this study, PI was calculated for each element and classified as low ( $PI \leq 1$ ), medium ( $1 < PI \leq 3$ ), or high ( $PI > 3$ ). IPI is obtained by calculating the geometric mean of the PI measurements of the relevant point for each element examined, and the results are classified as low ( $IPI \leq 1$ ), medium ( $1 < IPI \leq 2$ ) and high risk ( $IPI > 2$ ) [27].

Igeo was first proposed by [32] to compare pre-industrial and current heavy metal concentrations and is calculated by the following formula:

$$Igeo = \log_2 Cn / 1.5Bn$$

In the formula, Cn corresponds to the element concentration in the sample studied, and Bn corresponds to the average value in the upper crust / earth soil for the same element. In this study, upper crustal averages from [33] were used. A coefficient of 1.5 was proposed by [32] to balance possible effects on soils. [32] divided the Igeo parameter into seven classes between 0 – 6. According to this;

- < 0 = practically uncontaminated
- 0 – 1 = uncontaminated to moderately contaminated
- 1 – 2 = moderately contaminated
- 2 – 3 = moderately to strongly contaminated
- 3 – 4 = strongly contaminated
- 4 – 5 = strongly to extremely contaminated and
- > 5 = extremely contaminated

## 3. Results and discussion

### 3.1. Statistical evaluation of the data

[Table 1](#) presents the descriptive statistics of the 7 elements in the soil (mean, median, geometric mean, minimum, maximum and standard deviation). Elemental concentrations in soil are 10–265 ppm, 10–90 ppm; 15–545 ppm; 5–800 ppm; 2–60 ppm, 10 to 6300, and 15–1255 ppm for Cu, Pb, Zn, As, Sb, Ni and Co, respectively. The resulting concentrations generally exceed the expected upper crust values and uncontaminated soil values. The high concentrations at the sampling points are thought to be due to the Listwaenitization of ultramafic rocks because of hydrothermal alteration and metasomatism processes. The fact that the standard deviation values are different and larger than zero indicate that the sample populations deviate from the normal distribution, that is, there is a metal enrichment in the field. The environmental effects of element enrichment are discussed below with relevant pollution parameters.

Correlation coefficients were calculated ( $p \leq 0.05$  and  $p \leq 0.01$ ) in order to understand the co-behavior tendencies of the elements in the soil, and the multi-element correlation coefficients in the soil samples are given in [Table 2](#). Considering the multi-element correlation coefficients calculated for the elements, a positive significant relationship was found between Cu and Zn (0.75), between Sb and As (0.65), and between Ni and Co (0.73). The correlations detected between the elements were also found to be compatible with the behavioral associations of the elements.

### 3.2. Evaluation of the site with pollution parameters

Different assumptions can be used to calculate the IPI values of sampling points. For example, different IPI values are calculated for the elements related to each other by calculating the correlation coefficients, and IPI values are also calculated by considering the elements within the same factors by performing factor analysis for the examined elements, so that IPI values depending on the factors affecting the pollution in the researched area are determined. But, in this study, the IPI values of the sampling points were calculated by considering all the investigated elements / heavy metals.

Considering the IPI values calculated for the area, it has been determined that most of the sampling points in the area have a high risk of pollution, while relatively few sampling points have moderate pollution ([Fig. 2b](#)).

When the site was evaluated in terms of Cu according to the PI index, moderate pollution was detected in a significant part of the sampling points ([Fig. 2c](#)). Due to intense alteration, especially in areas close to tectonic

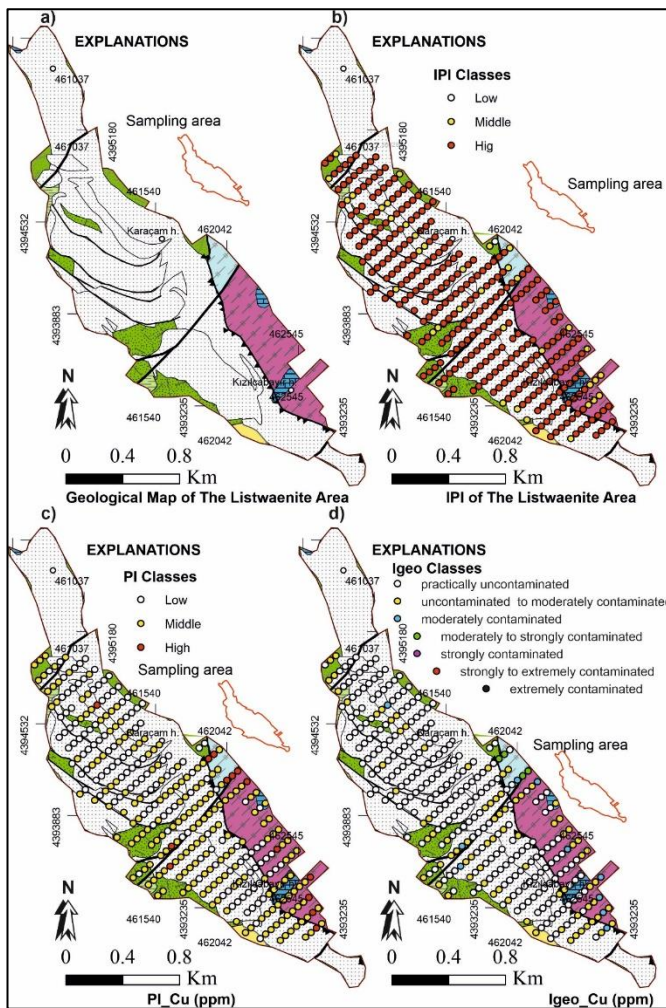


**Figure 2.** a) Study site geology map; b) Study site IPI dot map; c) PI Cu dot map; d) Igeo Cu dot map (See Fig. 1 for Figure explanation)

lines, high pollution, albeit limited, has been determined. Considering the Igeo index for copper, most of the site is practically uncontaminated, while the second plurality of sampling points falls into the uncontaminated to moderately polluted class. A small number of sampling points are in the moderately polluted class and a very small sampling point is in the moderate to severely polluted class (Fig. 2d).

When the site is evaluated with the PI parameter in terms of Pb element, it is seen that most of the sampling points are at the medium pollution level (Fig. 3a). High pollution was detected at only a few sampling points. When the site is evaluated with the Igeo index for Pb, most sampling points fall into the practically uncontaminated class, while a significant portion of the sampling points are in the uncontaminated to moderately polluted class. Only a few sampling points are moderately contaminated (Fig. 3b).

When the site is evaluated according to the PI index in terms of Zn, the southern part of the listwaenite zone is mostly observed in the medium pollution class, while the pollution level is mostly in the low class except for a few sampling points (Fig. 3c). There is high pollution at

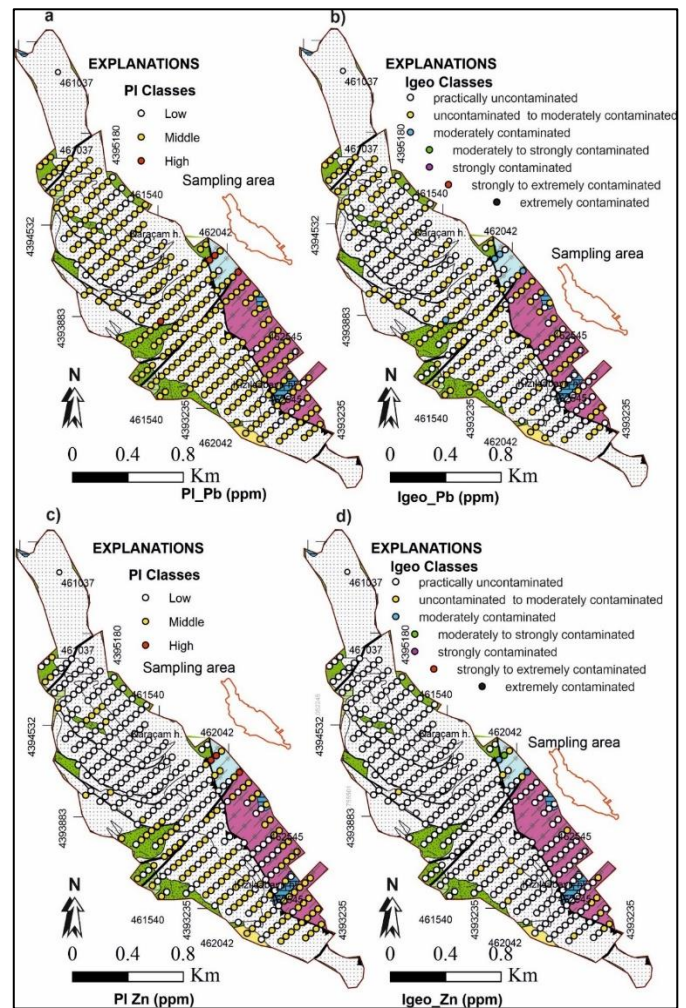


**Figure 3.** a) PI Pb dot map; b) Igeo Pb dot map; c) PI Zn dot map; d) Igeo Zn dot map (See Fig. 1 for Figure explanations)

only 3 points associated with tectonic lines, and when the site is evaluated in terms of Igeo index, most of the site is in the practically unpolluted class, while a small number of sampling points are in the unpolluted to moderately polluted class (Fig. 3d). Moderate pollution was determined at 2 sampling points and moderate to severely polluted class at one sampling point.

According to the PI parameter, the site is in the high pollution class in terms of arsenic (As) at many sampling points. It is seen that very few sampling points are in the medium pollution class (Fig. 4a). When the site is evaluated with the Igeo parameter for As, very few sampling points are in the practically uncontaminated class, with a few sampling points falling into the uncontaminated to moderately polluted class. Most of the sampling points fall into strongly to extremely contaminated class and extremely contaminated. A few sampling points are in the extremely contaminated class (Fig. 4b). In the light of these data, it has been determined that the site is remarkable in terms of pollution in terms of arsenic, and it is recommended to conduct a more detailed multi-purpose investigation in the area.

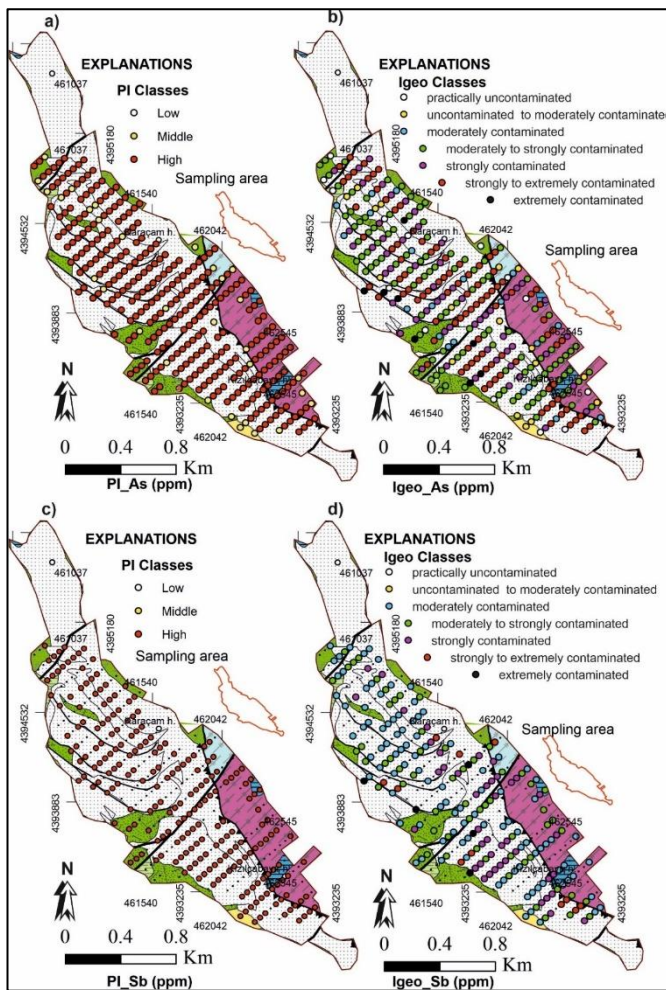


**Figure 4.** a) PI As dot map; b) Igeo As dot map; c) PI Sb dot map; d) Igeo Sb dot map (See Fig. 1 for Figure explanations)

When the study area is examined in terms of antimony, although the Sb was detected above the detection limit in fewer sampling points than the other elements, all sampling points are at high pollution level according to the PI parameter (Fig. 4c). When the Sb values in the field are evaluated with the Igeo parameter, most of the sampling points are in the moderately polluted class, while the remaining sampling points are respectively in the medium-strongly polluted, strongly polluted, and strongly-extremely polluted class (Fig. 4d). For Sb, only 5–6 sampling points are in the extremely polluted class.

When the site was evaluated with the PI index in terms of Ni element, high Ni pollution was detected at the points other than very few sampling points (Fig. 5a). Moderate contamination was detected at only a few sampling points. When the field is examined for Ni element in terms of Igeo parameter, it is determined that only a few sampling points are in the practically uncontaminated class and many sampling points in the south of the field fall into the extremely contaminated class (Fig. 5b). Other sampling points fall into the strongly to extremely contaminated class.

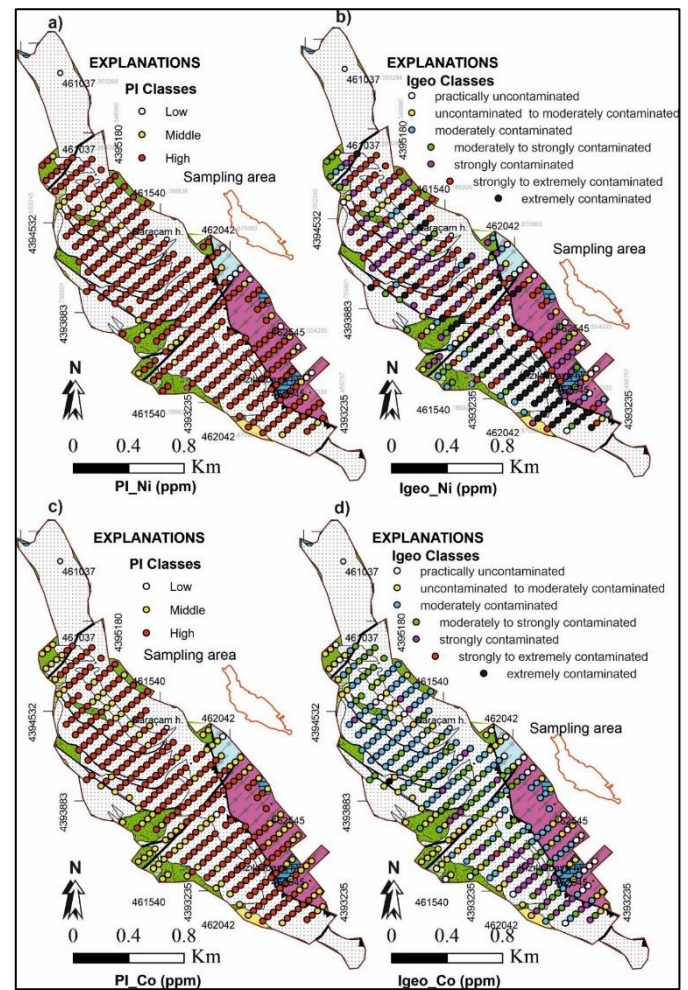


**Figure 5.** a) PI Ni dot map; b) Igeo Ni dot map; c) PI Co dot map; d) Igeo Co dot map (See Fig. 1 for Figure explanations)

When the study area is evaluated with the PI parameter in terms of Co, approximately 80% of the sampling point falls into the high pollution class. Only a few sampling points are in the low pollution class and about 15% of the sampling points are in the medium pollution class (Fig. 5c). When the field soils were evaluated with the Igeo parameter for Co contamination, it was determined that many of the sampling points were in the moderately polluted class and approximately 25% and 15% of the sampling points were moderately to strongly contaminated and strongly contaminated, respectively. Only 1–2 sampling points were found to be strongly to extremely contaminated and extremely contaminated (Fig. 5d).

### 3.3. Pollution parameters distribution maps

It was predicted that it would be useful to prepare distribution maps of pollution parameters for better evaluation of heavy metal pollution in the region, and thus distribution maps for PI, Igeo and IPI parameters of the listwaenite field were plotted. There are many methods in the plotting of distribution maps in spatial statistics studies. Considering the field conditions, the Kriging method was preferred for the study area. The Kriging method was first proposed by [34] and

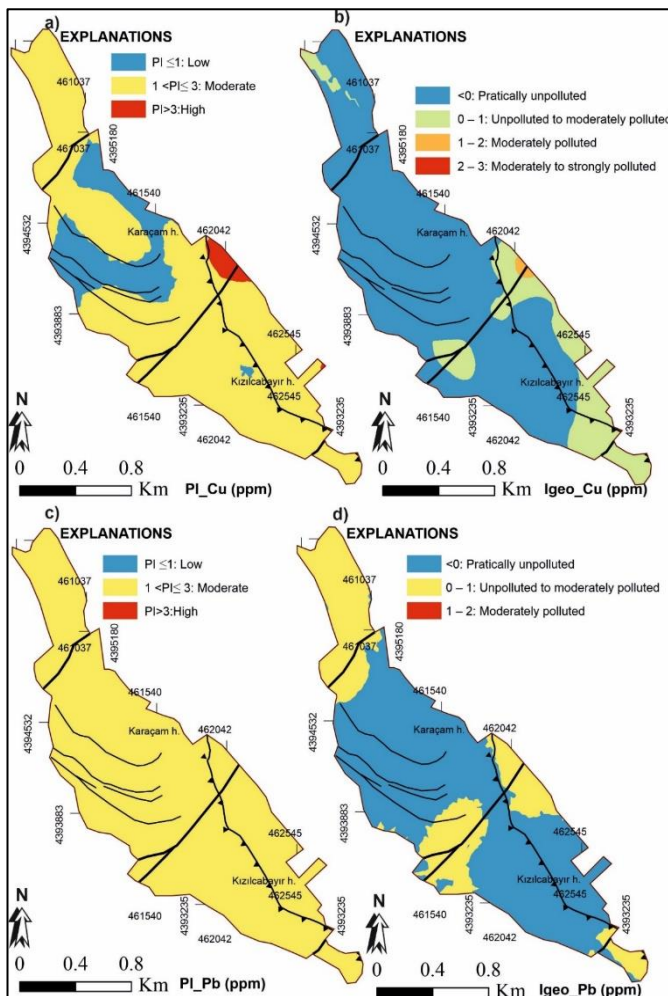


**Figure 6.** a) Distribution map of PI for Cu; b) Distribution map for Igeo of Cu; c) Distribution map of PI for Pb; d) Distribution map of Igeo for Pb (See Fig. 1 for Figure explanations)

developed by [35,36] and is widely used in spatial geostatistical interpolation studies. Kriging method is a flexible method that can be adjusted according to the situation by considering many parameters. It attempts to estimate unsampled point values using the information underlying the areal autocorrelation provided by the semi-variograms to find the most appropriate weighting sets to predict points and surfaces at sampling points. Because the semi-variogram is a function of distance, the weights vary according to the spatial distribution of the samples. Low weights are assigned to distant samples and higher weights are assigned to nearby samples. The Kriging method also considers the relative positions of the samples with respect to each other. Ordinary Kriging is the most reliable and can be easily used for many datasets. Although the transitions of the contours are smoother and more aesthetic in the Simple Kriging method, it is relatively less reliable. The Universal Kriging method, on the other hand, requires experience as well as having more data about the field. Considering all these data, Ordinary Kriging method was used to plot distribution maps of pollution parameters in the area.

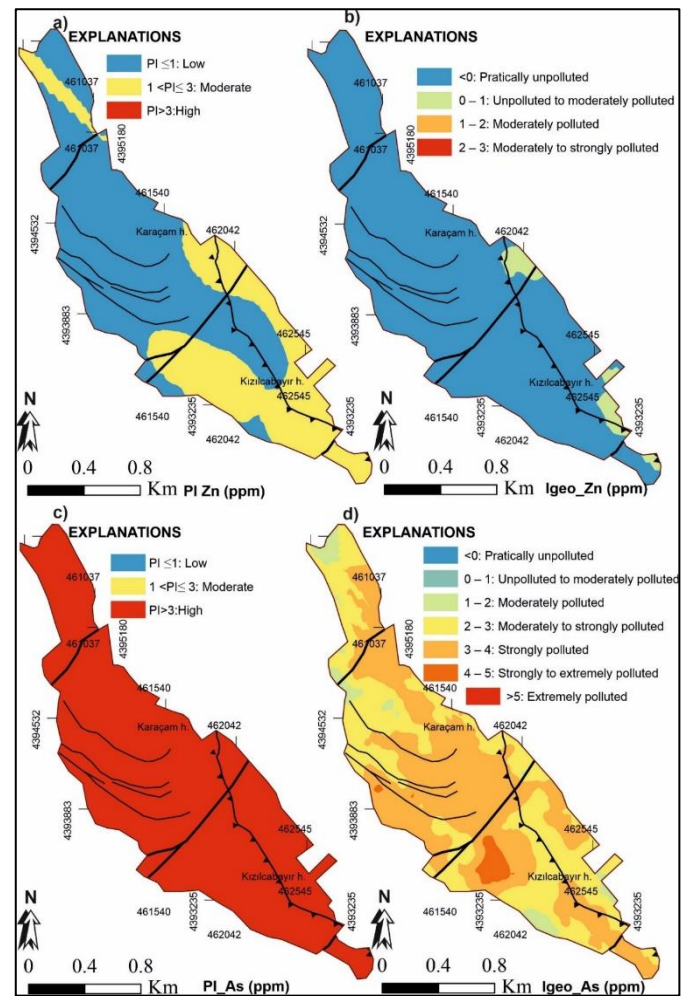


**Figure 7.** a) Distribution map of PI for Zn; b) Distribution map of Igeo for Zn; c) Distribution map of PI for As; d) Distribution map of Igeo for As (See Fig. 1 for Figure explanations)

Cross validation is used to investigate the accuracy of Kriging methods and to evaluate the performance of models used on the Kriging surface. In the studies carried out by many researchers, it has been seen that Kriging and Inverse Distance Weighting methods give the best performance in the studies where the number of points is not frequent and irregular sampling is performed, although most of the interpolation techniques give results close to each other and with high accuracy in regions with frequent sampling [37–46]. In this study, sampling points were organized regularly and frequently for heavy metals, distribution maps of PI, Igeo, and IPI parameters were plotted using the Ordinary Kriging and Constant method (Figs. 6–9).

When the PI distribution map of the copper element is examined (Fig. 6a), it is seen that a small part of the study area (Karaçam hill and its surroundings) shows low pollution, while a significant part of the area has medium pollution. It is seen that the immediate surroundings of the faulted contact separating the Kazdağ metamorphics and mylonitic gneiss have a high pollution risk. When the Igeo distribution map of Cu is examined, it is seen that most of the area is in the

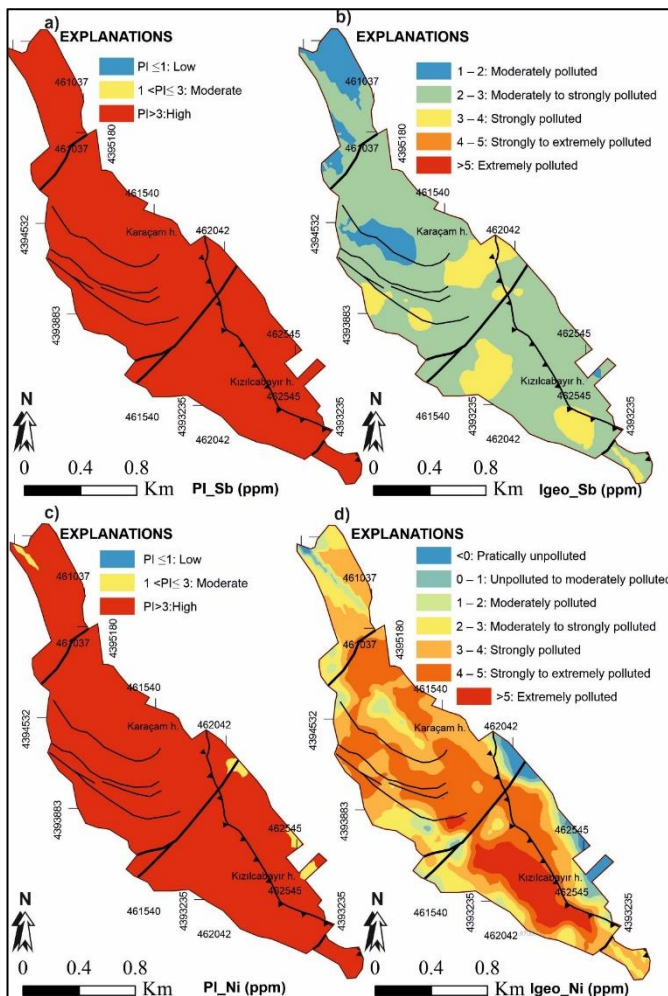


**Figure 8.** a) Distribution map of PI for Sb b) Distribution map of Igeo for Sb c) Distribution map of PI for Ni d) Distribution map of Igeo for Ni (See Fig. 1 for Figure explanations)

practically uncontaminated class, the southwestern part of the listwaenite zone, especially the part bordering the Kazdağ Group metamorphics, falls into the uncontaminated to moderately contaminated class, and the section with the fault contact separating the mylonitic gneiss and Kazdağ metamorphics is in the moderately contaminated class (Fig. 6b). This area partially coincides with the area falling into the high pollution risk class according to the PI parameter. When the PI distribution map for Pb is examined, the whole area is in the moderately polluted class (Fig. 6c). According to the distribution map of the Igeo parameter for Pb, it is seen that the sections with fault lines and relatively more severe alteration (northwest, southeast and middle part of the site) fall into the uncontaminated to moderately contaminated class. (Fig. 6d). According to the Igeo parameter, the areas remaining in the unpolluted to moderately polluted class for Cu and Pb are relatively overlapping areas (Fig. 6b and Fig. 6d).

When the PI distribution map for the Zn was examined, it was seen that a small area in the northwest and southeast of the field showed a medium pollution risk, while the rest had a low pollution risk (Fig. 7a).

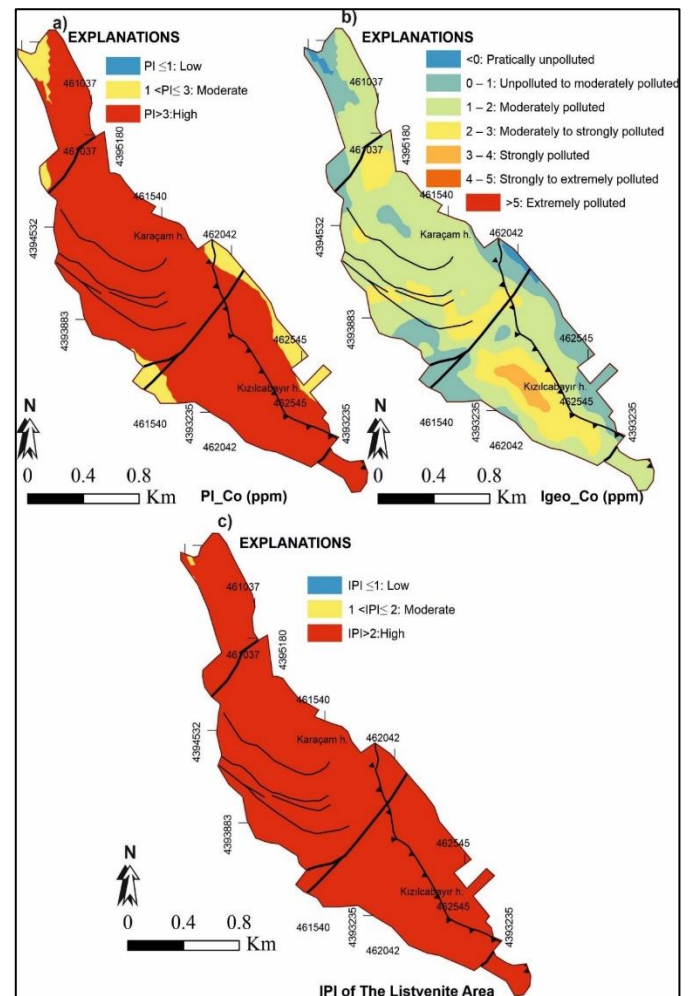


**Figure 9.** a) Distribution map of PI for Co, b) Distribution map of Igeo for Co, c) IPI distribution map for heavy metals (See Fig. 1 for Figure explanations)

According to the Igeo parameter for Zn, the distribution map shows that the limited areas in the southeast of Karaçam hill and east-southeast of Kızılcabayır hill are in the uncontaminated to moderately contaminated class, and the rest is in the practically uncontaminated class (Fig. 7b). According to the arsenic PI distribution map, the entire area shows a remarkably high pollution risk (Fig. 7c). According to the distribution map of the Igeo parameter, small areas in the northwest of the area and in the northwest of Karaçam hill fall into the moderately polluted class, while a significant part of the field falls into the moderately to strong polluted class and strongly polluted class. An area in the northwest of Kızılcabayır hill is classified as strongly to extremely polluted. Considering the PI and Igeo parameters for the field together, it is thought that it would be beneficial to study the field in more detail in terms of arsenic, both in soil and aquatic environments and in medical geology perspectives.

When the area was evaluated in terms of Sb, it was seen that the whole area fell into the high pollution risk class according to the PI distribution map (Fig. 8a). According to the distribution map of the Igeo parameter,

the field falls into the classes between moderately polluted and strongly polluted, and most of the field is in the moderately to strongly polluted class (Fig. 8b). When the field is examined in terms of Ni, almost all the field falls into the highly polluted class in the PI distribution map, while a very small portion falls into the moderate pollution risk class (Fig. 8c). According to the Igeo distribution map, very few parts of the area are in the practically unpolluted class, while the rest of the field falls between the moderately polluted and extremely polluted class. These remarkable pollution values observed in terms of Ni are related to the fact that the main rocks in the area are ultrabasic rocks in origin and the Ni element is not separated from the environment much and enriched in situ with the effect of lateritic processes. Especially since tectonic lines allow the movement of fluids, Ni pollution parameters are high in these areas (Fig. 8d).

When the Co PI distribution map is examined, it is determined that there is a medium pollution risk in small areas in the areas where listwaenite is bordered in other rocks, and a high pollution risk in the remaining section. In the Igeo distribution map, a very small part (northwest of the field, also southeast of Karaçam hill) is practically unpolluted, while most of the field is moderately polluted. Particularly in some parts close to tectonic lines, moderately to strongly polluted class was observed (Fig. 9b). To the west of Kızılcaşayır hill, there is an area that falls into the strongly polluted class. This area also partially overlaps with the Ni Igeo distribution map (Fig. 8d and Fig. 9b). This overlap is due to the similarity of the geochemical behavior characteristics of Ni and Co elements.

When the IPI distribution map of the study area is examined, it is seen that the entire area is in the highly polluted class (Fig. 9c). Therefore, the risk of heavy metal pollution caused by listwaenitization in the area was also confirmed by the IPI parameter. The IPI distribution map also confirms the need for more detailed investigation of the behavior and environmental effects of the elements in the field.

#### 4. Conclusions

The listwaenitization process, which is especially important for gold mineralization in terms of spatial and temporal, is also an enrichment for certain elements, in other words, it is a suitable environment for natural element pollution in relation to the hydrothermal events it is exposed to. Although there have been limited studies on the gold mineralization potential of the Alakeçi listwaenite field, there has been no study on the element / heavy metal pollution of the listwaenite in the

area. In this study, Cu, Pb, Zn, As, Sb, Ni and Co element concentrations of listwaenite-derived soils at Alakeçi listwaenite zone (Bayramiç / Çanakkale / Western Türkiye) were determined using flame atomic absorption spectrometry and the area was investigated in terms of heavy metal pollution with the help of PI, IPI and Igeo parameters, which are the most used in the evaluation of heavy metal pollution in soils. In addition, distribution maps of PI, Igeo and IPI parameters calculated for each element were plotted with the ordinary kriging constant method. As a result of the data obtained, it has been determined that there is a risk of pollution in the field in terms of PI and Igeo parameters, especially in the context of Ni, Co and As. Considering the IPI parameter, it has been determined that some of the sampling points in the field have a medium pollution risk, while many of the sampling points have a high pollution risk. When the distribution maps of the pollution parameters of the investigated elements are examined, it is seen that the pollution areas overlap in general, although the PI and Igeo pollution classifications of the elements differ. It has been determined that the areas showing pollution risk in the field correspond to tectonic lines and intense hydrothermal alteration areas. Element / heavy metal pollution caused by listwaenitization in the field poses risks both for terrestrial and aquatic environments and for human health through the food chain, especially in terms of As, Co and Ni. Therefore, it will be useful to carry out detailed research for environmental and medical geological purposes in the listwaenitization area.

#### Acknowledgements

The data used in this study were obtained within the scope of the mineral exploration project carried out by MTA and are the data used by the author in his doctoral thesis. The author would like to thank MTA and its project staff. The author also thanks Prof Dr Abdullah Kaygusuz for his encouragement in the preparation of this article on heavy metal pollution due to listwaenitization.

#### References

- [1] A. Vural, D. Aydal, Soil geochemistry study of the listwaenite area of Ayvacık (Çanakkale, Turkey), *Casp J Environ Sci*, 18, 2020, 205–215.
- [2] A. Vural, Bayramiç (Çanakkale) ve Çevresindeki Altın Zenginleşmelerinin Araştırılması, Ankara Üniversitesi, 2006.
- [3] R. Murchission, E. de Verneuil, A. Von Seyserling, The geology of Russia in Europe and the Ural Mountains. Geology, John Murray, 1845, London, UK.

- [4] B. Zoheir, Transpressional zones in ophiolitic melange terranes: Potential exploration targets for gold in the South Eastern Desert, Egypt, *J. Geochemical Explor*, 111, 2011, 23–38.
- [5] D. Béziat, M. Dubois, P. Debat, S. Nikiéma, S. Salvi, F. Tollon, Gold metallogeny in the Birimian craton of Burkina Faso (West Africa), *J African Earth Sci*, 50, 2008, 215–233.
- [6] E.V. Belogub, I.Y. Melekestseva, K.A. Novoselov, M. V. Zabolina, G.A. Tret'yakov, V.V. Zaykov, A.M. Yuminov, Listvenite-related gold deposits of the South Urals (Russia): A review, *Ore Geol Rev*, 85, 2017, 247–270.
- [7] A. Aftabi, M.H. Zarrinkoub, Petrogeochemistry of listvenite association in metaophiolites of Sahlabad region, eastern Iran: Implications for possible epigenetic Cu-Au ore exploration in metaophiolites, *Lithos*, 156–159, 2013, 186–203.
- [8] Ş. Koç, Y. Kadioğlu, Mineralogy, geochemistry and precious metal content of Karacakaya listwaenites, Turkey, *Ophioliti*, 21, 1996, 125–130.
- [9] D. Aydal, Gold-bearing listwaenites in the Arac Massif, Kastamonu, Turkey, *Terra Nov*, 2, 1990, 43–52.
- [10] T. Hinsken, M. Bröcker, H. Strauss, F. Bulle, Geochemical, isotopic and geochronological characterization of listvenite from the Upper Unit on Tinos, Cyclades, Greece, *Lithos*, 282–283, 2017, 281–297.
- [11] B. Zoheir, B. Lehmann, Listvenite-lode association at the Barramiya gold mine, Eastern Desert, Egypt, *Ore Geol Rev*, 39, 2011, 101–115.
- [12] B.R. Frost, K.A. Evans, S.M. Swapp, J.S. Beard, F.E. Mothersole, The process of serpentinization in dunite from new caledonia, *Lithos*, 178, 2013, 24–39.
- [13] M. Yusuf, M. Kumar, M.A. Khan, M. Sillanpa, H. Arafat, Hydrothermal listvenitization and associated mineralizations in Zagros Ophiolites: Implications for mineral exploration in Iraqi Kurdistan, *J Geochemical Explor*, 2019, 102036.
- [14] M. Ahankoub, M.A. Mackizadeh, Mineralogy and geochemistry of the Dehshir listvenites, central Iran, *Neues Jahrb Fur Mineral Abhandlungen*, 196, 2019, 1–18.
- [15] C. Hall, R. Zhao, Listvenite and related rocks: perspectives on terminology and mineralogy with reference to an occurrence at Cregganbaun, Co. Mayo, Republic of Ireland, *Miner Deposita*, 30, 1995, 303–313.
- [16] H.A. Gahlan, M.K. Azer, P.D. Asimow, K.M. Al-Kahtany, Formation of gold-bearing listvenite in the mantle section of the Neoproterozoic Bir Umq ophiolite, Western Arabian Shield, Saudi Arabia, *J African Earth Sci*, 190, 2022, 104517.
- [17] A.D. Kiliç, M. İnceöz, Mineralogical, geochemical and isotopic effect of silica in ultramaphic systems, eastern Anatolian Turkey, *Geochemistry Int*, 53, 2015, 369–382.
- [18] Y. Yang, L. Zhao, R. Zheng, Q. Xu, Evolution of the early Paleozoic Hongguleleng–Balkybye Ocean: Evidence from the Hebukesaier ophiolitic mélange in the northern West Junggar, NW China, *Lithos*, 324–325, 2019, 519–536.
- [19] A. Vural, Contamination assessment of heavy metals associated with an alteration area: Demirören Gumushane, NE Turkey, *J. Geol Soc India*, 86, 2015, 215–222.
- [20] G. Külekçi, Investigation of gamma ray absorption levels of composites produced from copper mine tailings, fly ash, and brick dust, *J Mater Cycles Waste Manag*, 24, 2022, 1934–1947.
- [21] G. Külekçi, Investigation of fly ash added light concretes with respect to gamma radiation transmission properties of <sup>133</sup>Ba and <sup>137</sup>Cs, *Radiat Eff Defects Solids*, 176, 2021, 833–844.
- [22] A. Vural, D. Aydal, Determination of lithological differences and hydrothermal alteration areas by remote sensing studies: Kısacık (Ayvacık-Çanakkale, Biga Peninsula, Turkey), *J Eng Res Appl Sci*, 9, 2020, 1341–1357.
- [23] G. Külekçi, <sup>60</sup>Co Radyoaktif Nokta Kaynağı ile Uçucu Külün Gama Radyasyon Koruma Özellikleri, *Avrupa Bilim ve Teknol Derg*, 27, 2021, 145–151.
- [24] A.İ. Okay, M. Siyako, K.A. Burkan, Geology and tectonic of the Biga Peninsula, *Turk Assoc Pet Geol Bull*, 2, 1990, 83–121.
- [25] A.W. Rose, H. Hawkes, J. Webs, *Geochemistry in Mineral Exploration*, 2nd ed., Academic Press, 1991, London, England.
- [26] D. Skoog, D. West, F. Holler, S. Crouch, *Fundamentals of analytical chemistry*, 8th ed., Brooks/Cole-Thomson Learning, Belmont, CA 94002, 2004, USA.
- [27] C.W. Chen, C.M. Kao, C.F. Chen, C. Di Dong, Distribution and accumulation of heavy metals in the sediments of Kaohsiung Harbor, Taiwan, *Chemosphere*, 66, 2007, 1431–1440.
- [28] B.T. Sany, A. Salleh, A.H. Sulaiman, A. Mehdinia, G.H. Monazami, *Geochemical Assessment of Heavy Metals Concentration in Surface Sediment of West Port, Malaysia*, 5(8), 2011, 411–415.
- [29] Ü. Gemici, Evaluation of the water quality related to the acid mine drainage of an abandoned mercury mine (Alaşehir, Turkey), *Environ Monit Assess*, 147, 2008, 93–106.
- [30] A. Sungur, M. Soylak, H. Özcan, Chemical fractionation, mobility and environmental impacts of heavy metals in greenhouse soils from Çanakkale, Turkey, *Environ Earth Sci*, 75, 2016, 1–11.
- [31] G. Yaylali-Abanuz, Determination of anomalies associated with Sb mineralization in soil geochemistry: A case study in Turhal (northern Turkey), *J Geochemical Explor*, 132, 2013, 63–74.
- [32] G. Muller, Index of geoaccumulation in sediments of the Rhine River, *Geol J*, 2, 1969, 108–118.
- [33] R. Rudnick, S. Gao, Composition of the Continental Crust, in: H. Holland, K. Turekian (Eds.), *Readings of Treatise on Geochemistry*, 2nd ed., Elsevier, 2010, London, England.
- [34] D.G. Krige, A statistical Approach to Some Basic Mine Valuation Problems on the Witwatersrand, *J Chem Metall Soc South Min Africa*, 52, 1951, 119–139.
- [35] G. Matheron, Principles of geostatistics, *Econ Geol*, 58, 1963, 1246–1266.
- [36] G. Matheron, *The Theory of Regionalized Variables and Its Applications*, École nationale supérieure des mines, 1971, Paris.
- [37] M. Akçay, A. Lermi, A. Van, Biogeochemical exploration for massive sulphide deposits in areas of dense vegetation: An orientation survey around the Kankoy Deposit, *J Geochemical Explor*, 63, 1998, 173–187.
- [38] N. Ağca, Spatial distribution of heavy metal content in soils around an industrial area in Southern Turkey, *Arab J Geosci*, 8, 2015, 1111–1123.
- [39] C. Patinha, E. Correia, E. Ferreira da Silva, A. Simões, P. Reis, F. Morgado, E. Cardoso Fonseca, Definition of geochemical patterns on the soil of Paul de Arzila using correspondence analysis, *J Geochemical Explor*, 98, 2008, 34–42.
- [40] G. Buttafuoco, A. Tallarico, G. Falcone, I. Guagliardi, A geostatistical approach for mapping and uncertainty assessment of geogenic radon gas in soil in an area of southern Italy, *Environ Earth Sci*, 61, 2010, 491–505.
- [41] M. Basaran, G. Erpul, A.U. Ozcan, D.S. Saygin, M. Kibar, I. Bayramin, F.E. Yilman, Spatial information of soil hydraulic conductivity and performance of cokriging over kriging in a semi-arid basin scale, *Environ Earth Sci*, 63, 2011, 827–838.
- [42] R. Webster, M.A. Oliver, *Geostatistics for Environmental Scientists*, 2nd ed., Jhon Wiley&Sons Ltd., 2007.
- [43] T. Hengl, *A Practical Guide to Geostatistical Mapping of Environmental Variables*, 2007.
- [44] A. Vural, M. Erdoğan, Eski Gümüşhane Kırkpavli alterasyon sahasında toprak jeokimyası, *Gümüşhane Üniversitesi Fen Bilim Enstitüsü Derg*, 4, 2014, 1–15.
- [45] A. Vural, B. Çiçek, Çevreleşme Sahasında Gelişmiş Topraklardaki Ağır Metal Kirliliği, *Düzce Üniversitesi Bilim ve Teknol Derg*, 8, 2020, 1533–1547.
- [46] V. Chaplot, F. Darboux, H. Bourennane, S. Leguédou, N. Silvera, K. Phachomphon, Accuracy of interpolation techniques for the derivation of digital elevation models in relation to landform types and data density, *Geomorphology*, 77, 2006, 126–141.